Acta Crystallographica Section B
Structural Science
ISSN 0108-7681

Structure correlation study of four-coordinate copper(I) and (II) complexes

Paul R. Raithby,[a]* Gregory P. Shields,[a,b] Frank H. Allen[b] and W. D. Samuel Motherwell[b]

[a]Department of Chemistry, Lensfield Road, Cambridge CB2 1EW, England, and [b]Cambridge Crystallographic Data Centre, 12 Union Road, Cambridge CB2 1EZ, England

Correspondence e-mail: prr1@cam.ac.uk

Received 15 June 1999
Accepted 24 December 1999

The geometries of four-coordinate Cu^{I} and Cu^{II} complexes in the Cambridge Structural Database (CSD) have been analysed systematically and compared using symmetry-deformation coordinates and principal component analysis. The observed stereochemistries have been rationalized in terms of the *d*-electron configurations, interligand repulsion and π-bonding effects. The results confirm that the majority of four-coordinate copper(I) complexes in the CSD adopt tetrahedral geometries and deviations from tetrahedral symmetry are caused by the presence of chelating ligands or by the incorporation of copper centres into dimeric or polymeric structures. Four-coordinate copper(II) complexes generally adopt geometries close to square planar; this is particularly evident for *bis*(chelate) complexes where π-bonding is important. Distortions towards tetrahedral geometries are attributable to steric interactions of bulky substituents in the bidentate ligands.

1. Introduction

The coordination chemistry of copper in its +I, +II and less common +III oxidation states has been extensively studied and has been the subject of many annual literature reviews (*e.g.* Smith, 1997*a*,*b*, 1998) and reports (Smith, 1995, 1996, 1997). Holloway & Melnik (1995) have published a comprehensive survey and tabulation of the structural data available for copper(I) compounds published up to 1992, providing a detailed analysis and rationalization of the observed geometries. However, they did not attempt to correlate the observed stereochemistries using statistical or numerical methods, nor did they describe the bond-length and -angle deformations using symmetry-deformation coordinates. More recently, Melnik *et al.* (1997) have published similar surveys of mononuclear four- and five-coordinate copper(II) and binuclear copper(II) complexes (Melnik *et al.*, 1998).

It is now well established that copper(I) has a d^{10} electronic configuration which is stereochemically inactive and coordination numbers of 2 (linear), 3 (trigonal planar) and 4 (tetrahedral) are the most common (Holloway & Melnik, 1995). Copper(II), with the d^{9} electronic configuration, exhibits a wider range of stereochemistries, with four-coordinate complexes spanning approximately tetrahedral (T_d), compressed tetrahedral (D_{2d}) and square-coplanar (D_{4h}) geometries (Hathaway & Billing, 1970; Gazo *et al.*, 1976; Hathaway *et al.*, 1981; Hathaway, 1981, 1982). The chemistry of d^{8} Cu^{III} is dominated by the square-coplanar configuration.

The ^{2}E electronic ground state in the tetrahedral copper(II) geometry is orbitally degenerate and subject to a Jahn–Teller

(Jahn & Teller, 1937) distortion removing that degeneracy. Whilst this degeneracy may be removed by spin-orbit coupling, the resulting states are close in energy and an angular deformation often occurs towards a square-planar geometry. π-bonding in the equatorial plane is probably necessary for the formation of square-planar complexes, since axial contacts (particularly to ligands with some π-bonding potential) are usually needed if planarity is otherwise to be maintained. Whereas distortion towards the planar geometry aligns the ligands so as to interact most strongly with the half-filled *d*-orbital, thus minimizing *d*-electron to ligand–electron repulsion, the planar geometry brings the ligand donor atoms into closer proximity, which increases ligand–ligand inter-electron repulsion, provided that the ligand–metal bonding is not strongly directional, *i.e.* is electrostatic or primarily involves *s* orbitals on the ligands and the 4*s* orbital on the Cu. If there is a strong contribution from the copper 4*p* orbitals, or a significant π-bonding contribution (involving copper 4*p* or 3*d* orbitals), the planar geometry may be stabilized. The short equatorial bonds in the planar acac and salim complexes arise from the combined effect of strong, short, σ-bonds and π-back-donation from the copper d_{xz} and d_{yx} orbitals into anti-bonding orbitals on the ligand (Pauling, 1940).

Klebe & Weber (1994) investigated interconversion pathways between tetrahedral and square-planar stereochemistries for a number of metal ions, using the structure correlation approach of Bürgi & Dunitz (1991; Auf der Heyde & Bürgi, 1989). The coordination geometries of Cu fragments retrieved from the Cambridge Structural Database (CSD; Allen & Kennard, 1993) were analysed using symmetry-deformation coordinates (SDCs; Murray-Rust *et al.*, 1979) referred to an idealized tetrahedral geometry (Fig. 1), and mapped into the 3*m* sub-space spanned by the S_{2a} (tetragonal compression) and S_{2b} (diagonal twist) SDCs (Table 1, Fig. 2; Murray-Rust *et al.*, 1978*a*; Muetterties & Guggenberger, 1974).

Two reaction coordinates were discussed for four-coordinate copper complexes. A tetragonal compression along S_{2a} was suggested for Cu centres coordinated by four monodentate ligands. The second involved an elongation along S_{2a}, followed by a diagonal twist to a rectangular planar arrangement and a compression in the equatorial plane to produce the square-planar geometry. It was suggested that complexes with bidentate chelating ligands might follow the latter mechanism, since the restricted bite angle of the ligands would favour elongation and reduce repulsion between donor atoms in facing ligands undergoing a twist-type deformation. A series of structures from the CSD was used in each case to illustrate points along these reaction coordinates.

The CSD only stores oxidation state information if it was given in the original publication (Cambridge Structural Database, 1992). Furthermore, the oxidation state is included in the text of the compound name field and not identified with a particular metal centre, so may not be used as a substructure search criterion. As a result, Klebe & Weber (1994) were unable to automatically take account of the formal oxidation state of the metals involved in their study; no distinction was made between d^8 Cu^{III}, d^9 Cu^{II} or d^{10} Cu^{I} complexes, despite their different stereoelectronic preferences. Of the complexes used to illustrate the tetrahedral compression pathway, all were Cu^{II} complexes possessing halogen ligands with the exception of the tetrahedral example which was Cu^{I}. For the diagonal twist coordinate, the eight examples most closely approaching tetrahedral geometry were Cu^{I}, whilst the remainder were either Cu^{II} or Cu^{III}.

In this paper, we reinterpret the crystallographic data for well determined four-coordinate copper compounds available in the CSD, taking oxidation state into account. This enables the observed geometries of four-coordinate Cu^{I} and Cu^{II} complexes to be analysed and compared in a general manner using SDCs and principal component analysis (PCA: Chatfield & Collins, 1980; Murray-Rust & Bland, 1978). Whilst this methodology does not enable detailed effects to be examined at the individual structure level (as in the analyses of Holloway & Melnik, 1995, and Melnik *et al.*, 1997, 1998) it does demonstrate the overall trends more clearly. Conversely, it provides more information on the nature of the distortion pathway than methods which provide a single parameter to quantify the overall distortion, *e.g.* continuous symmetry (Pinsky & Avnir, 1998), symmetry-constrained RMS (root-mean square) deviation (Dollase, 1974), polyhedral volume (Makovicky & Balic Zunic, 1998) or angle-based methods (Howard *et al.*, 1998). As a result, the observed stereochemistries may be rationalized in terms of the *d*-electron

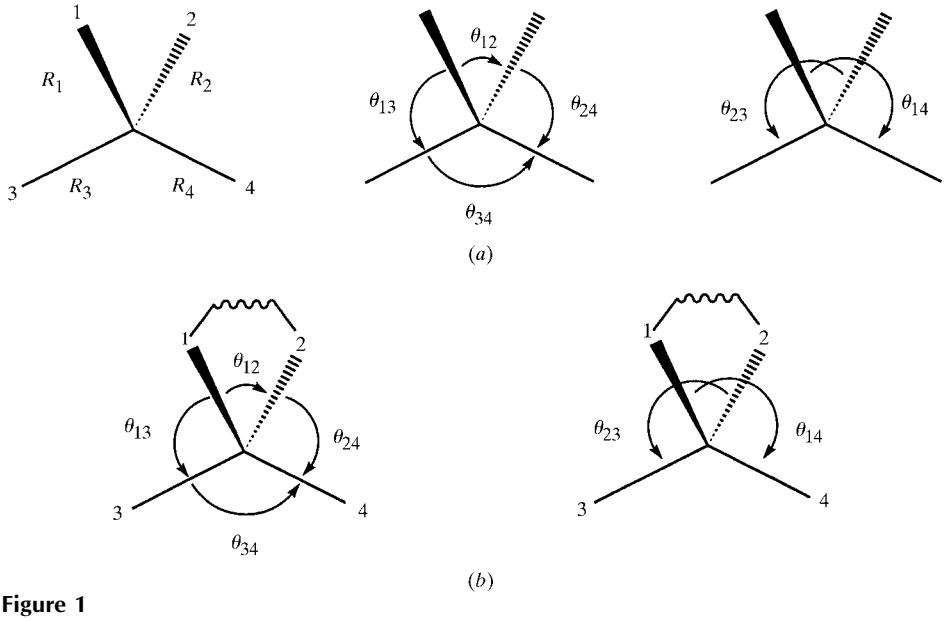

Figure 1
Internal coordinates for (*a*) T_d reference geometry and (*b*) C_{2v} Cu(LL)$L'L''$ reference geometry.

Table 1
Symmetry-deformation coordinates (SDCs) for four-coordinate tetrahedral reference geometry (T_d).

SDC	IR	Kernel	Co-kernel
$S_1 = \frac{1}{2}(\delta R_1 + \delta R_2 + \delta R_3 + \delta R_4)$	A_1	T_d	
$S_{2a} = \frac{1}{(12)^{1/2}}(2\delta\theta_{12} - \delta\theta_{13} - \delta\theta_{14} - \delta\theta_{23} - \delta\theta_{24} + 2\delta\theta_{34})$	E	D_2	D_{2h}
$S_{2b} = \frac{1}{2}(\delta\theta_{13} - \delta\theta_{14} - \delta\theta_{23} + \delta\theta_{24})$	E	D_2	
$S_{3a} = \frac{1}{2}(\delta R_1 + \delta R_2 - \delta R_3 - \delta R_4)$	T_2	C_1	C_{2v}
$S_{3b} = \frac{1}{2}(\delta R_1 - \delta R_2 + \delta R_3 - \delta R_4)$	T_2	C_1	C_{2v}
$S_{3c} = \frac{1}{2}(\delta R_1 - \delta R_2 - \delta R_3 + \delta R_4)$	T_2	C_1	C_{2v}
$S'_{3a} = \frac{1}{(12)^{1/2}}(3\delta R_1 - \delta R_2 - \delta R_3 - \delta R_4)$	T_2	C_1	C_{3v}
$S'_{3b} = \frac{1}{(6)^{1/2}}(2\delta R_2 - \delta R_3 - \delta R_4)$	T_2	C_1	C_s
$S'_{3c} = \frac{1}{(2)^{1/2}}(\delta R_3 - \delta R_4)$	T_2	C_1	C_s
$S_{4a} = \frac{1}{(2)^{1/2}}(\delta\theta_{12} - \delta\theta_{34})$	T_2	C_1	C_{2v}
$S_{4b} = \frac{1}{(2)^{1/2}}(\delta\theta_{13} - \delta\theta_{24})$	T_2	C_1	C_{2v}
$S_{4c} = \frac{1}{(2)^{1/2}}(\delta\theta_{14} - \delta\theta_{23})$	T_2	C_1	C_{2v}
$S'_{4a} = \frac{1}{(6)^{1/2}}(\delta\theta_{12} + \delta\theta_{13} + \delta\theta_{14} - \delta\theta_{23} - \delta\theta_{24} - \delta\theta_{34})$	T_2	C_1	C_{3v}
$S'_{4b} = \frac{1}{(6)^{1/2}}(2\delta\theta_{12} - \delta\theta_{13} - \delta\theta_{14} + \delta\theta_{23} + \delta\theta_{24} - 2\delta\theta_{34})$	T_2	C_1	C_{5v}
$S'_{4c} = \frac{1}{2}(\delta\theta_{13} - \delta\theta_{14} + \delta\theta_{23} - \delta\theta_{24})$	T_2	C_1	C_s
$S_5 = \frac{1}{(6)^{1/2}}(\delta\theta_{12} + \delta\theta_{13} + \delta\theta_{14} + \delta\theta_{23} + \delta\theta_{24} + \delta\theta_{34})$	A_1	T_d	(R)

(R) S_5 is formally redundant

configurations, inter-ligand repulsion and π-bonding effects discussed above.

2. Experimental

2.1. Data retrieval

A CSD *QUEST*3D search (April 1995 release, 140 270 entries) was made for Cu complexes having exactly four single bonds to non-metal donor atoms, specified as X = B, C, N, O, F, Si, P, S, Cl, As, Se, Br, Te and I. This yielded 1320 entries, excluding structures having bond-length errors > 0.02 Å, an R factor $\geq$ 10% or no atomic coordinates stored. Subsequently, duplicate determinations of the same compound were retained only where these represented different polymorphs, otherwise only the room-temperature X-ray diffraction structure (where available) with the lowest R factor was retained.

Copper(II) centres which were not genuinely four-coordinate were also rejected. Complexes with additional semi-coordinated (Brown *et al.*, 1967) axial donor atoms, within 0.75 Å of the sum of the respective covalent radii, were located with a *QUEST*3D non-bonded contact search. The CSD default elemental radii (Cambridge Structural Database, 1994) were used and both intermolecular and intramolecular Cu$\cdots X$ contacts were located in the search. In the intramolecular case, non-metal atoms (X) were required to be four or more bonds removed from Cu. In addition, we rejected four-coordinate fragments having intramolecular non-bonded contacts < 3 Å to O or N donor atoms, which were only three bonds removed from Cu in complexes containing asymmetrically bidentate ligands with small bite angles, *e.g.* carboxylate and nitrate complexes, since these are more properly considered as being [4 + 2]-coordinate (*i.e.* with two additional semi-coordinated axial ligands).

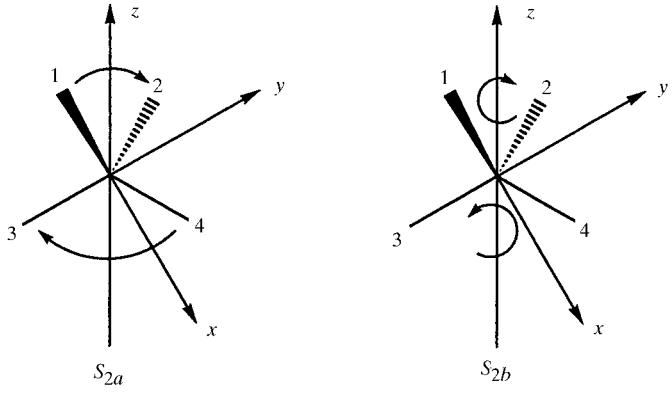

Figure 2
Tetragonal compression and diagonal twist coordinates describing deformations from T_d symmetry, maintaining D_{2d} and D_2 symmetry, respectively.

2.2. Oxidation state assignment

The resulting subset was investigated manually and the entries sorted according to Cu oxidation state. The oxidation state specified in the compound name field was used as the primary criterion. Where there was any doubt as to the correct assignment of an oxidation state, the structure was excluded from further analysis. These procedures resulted in subsets of 346 and 414 structures comprising 445 and 460 unique Cu centres for Cu^{I} and Cu^{II}, respectively.

2.3. Bond length and angle deformations

An appropriate standard bond length is necessary if deformations involving different donor atoms are to be compared directly. A previous tabulation of transition-metal–non-metal bond lengths provided distances which were specific to particular classes of ligands, although not necessarily to a metal atom in a particular oxidation state (Orpen *et al.*, 1989). For our study, mean (unweighted) ligand–metal bond lengths and their standard deviations were calculated for each donor atom type from the structures in the Cu^{I} and Cu^{II} subsets. The results, along with values derived from the default radii available in the CSD (where the same radius is used for both Cu^{I} and Cu^{II}) for comparison, are shown in Table 2 for both Cu^{I} and Cu^{II}. For some elements there were too few observations for the calculated mean bond lengths to be a reliable estimate of the true mean values and approximate values for these elements were derived by interpolation based on the CSD bonding radii. Since bonds to these elements comprise only a small fraction of each data set, their precise values did not significantly influence the subsequent statistical

Table 2
Representative bond lengths in four-coordinate Cu^{I} and Cu^{II} complexes.

		C	N	O	Si	P	S	Cl	As	Se	Br	I
Cu^{I}	Observations	37	466	48	1†	334	288	100	16	6†	89	115
	$\bar{x}_u$	1.876	2.057	2.134	2.333	2.279	2.338	2.425	2.383	2.408	2.524	2.678
	$\sigma(\bar{x}_u)$	0.014	0.003	0.020	–	0.003	0.005	0.015	0.009	0.008	0.008	0.006
	σ_i	0.082	0.075	0.137	–	0.053	0.091	0.153	0.036	0.020	0.072	0.063
	Distance used for normalization	1.88	2.06	2.13	2.30	2.28	2.34	2.42	2.38	2.40	2.52	2.68
Cu^{II}	Observations	–	851	688	–	3†	120	156	–	4†	37	1†
	$\bar{x}_u$	–	1.973	1.911	–	2.186	2.267	2.250	–	2.365	2.377	2.554
	$\sigma(\bar{x}_u)$	–	0.002	0.001	–	0.003	0.004	0.005	–	0.0	0.007	–
	σ_i	–	0.046	0.030	–	0.005	0.049	0.057	–	0.0	0.045	–
	Distance used for normalization	–	1.97	1.91	–	2.30	2.27	2.25	–	2.40	2.38	2.55
	CSD values‡	–	2.20	2.20	–	2.57	2.54	2.51	–	2.74	2.73	2.92

† Too few observations for the mean value to be reliable. ‡ Values derived from the default CSD bonding radii.

analyses and they did not appear as outliers in the normalized bond length distributions. Bond length deformations, δR *etc.* were then evaluated relative to these standard values.

For the tetrahedral reference geometry used for Cu^{I}, displacements from the tetrahedral angle of 109.471° were multiplied by the factor 0.039, thus converting the angular displacement to the arc-length described at a radius of 2.25 Å (typical Cu^{I}—L bond length). For the D_{4h} square-planar Cu^{II} reference (Fig. 3), the angular deformation coordinates were calculated as follows:

$$\delta\theta_{ij} = 0.035(A_{ij} - 90) \quad (ij = 12, 13, 14, 23) \tag{1}$$

$$\delta\theta_{kl} = 0.035(A_{kl} - 180) \quad (kl = 24, 34), \tag{2}$$

where 0.035 is the scaling factor to convert angular displacements to Å, equivalent to the arc length described when a vector of average Cu^{II}—L bond length r = 2.00 Å moves through an angle $\delta\theta$ of 1°.

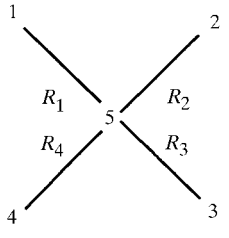

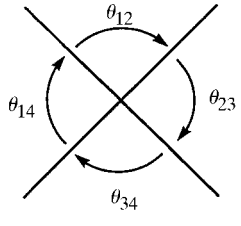

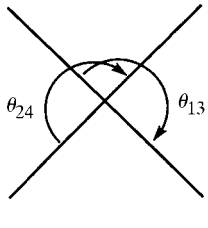

Atom permutational operators:

5	1	2	3	4
5	2	3	4	1
5	3	4	1	2
5	4	1	2	3
5	4	3	2	1
5	3	2	1	4
5	2	1	4	3
5	1	4	3	2

Bond permutational operators:

1	2	3	4
2	3	4	1
3	4	1	2
4	1	2	3
4	3	2	1
3	2	1	4
2	1	4	3
1	4	3	2

Angle permutational operators:

12	23	34	14	13	24
23	34	14	12	24	13
34	14	12	23	13	24
14	12	23	34	24	13
34	23	12	14	24	13
23	12	14	34	13	24
12	14	34	23	24	13
14	34	23	12	13	24

Figure 3
Internal coordinates for D_{4h} reference geometry.

The search condition that θ_{24} was the largest angle ensured that the desired atom mapping, with the atom pairs 1,3 and 2,4 *trans*, was found. Although θ_{13} and θ_{24} are defined (Fig. 3) with respect to the same side of the (x, y) plane, the values returned in the output geometry table are always $\leq$180°. As a result, they give no account of sense and the angle deformations would always have a negative sign. However, if the complex adopts a pyramidal configuration, $\delta\theta_{13}$ and $\delta\theta_{24}$ have the same sign, whereas if it becomes more tetrahedral, $\delta\theta_{13}$ and $\delta\theta_{24}$ have opposite signs. To take account of this, the sign of $\delta\theta_{24}$ (angle θ_{24} being the nearest to 180°) was reversed if ($\theta_{12} + \theta_{23} + \theta_{34} + \theta_{14}$) was greater than 360° (reversing the sign of θ_{13} rather than θ_{24} would generate the other enantiomer).

2.4. Symmetry-deformation coordinates and principal component analysis

The normalized datasets were symmetry-permuted and SDCs calculated using local code. For the general Cu^{I} dataset, a 24-fold permutation was applied, appropriate for the T_d reference fragment, whereas for the $Cu^{I}(LL)L'L''$ dataset, fourfold expansion consistent with ideal C_{2v} $Cu(LL)L_2'$ symmetry was employed. After symmetry permutation, the initial Cu^{I} subset comprised too many fragments for analysis in the CSD package *VISTA*, so the search was restricted further to structures with R factors < 7.5%, producing 299 hits and 375 unique Cu^{I} fragments. The Cu^{II} dataset was 16-fold permuted to fill the D_{4h} permutational space, by including both enantiomers (signs of $\delta\theta_{12}$ and $\delta\theta_{24}$ reversed) for each of the eight topological mappings for the purpose of PCA analysis. However, only one enantiomer was used for the SDC plots, resulting in a data set with a symmetry that is characteristic of a C_{4v} rather than D_{4h} reference structure (since the definition adopted for θ_{13} and θ_{24} arbitrarily restricts out-of-plane deformations to one direction).

The resulting geometry tables were imported into *VISTA* for PCA (Chatfield & Collins, 1980) and statistical analyses. Three-dimensional scatterplots were produced using the program *PLOTMTV* (Toh, 1994). Expanding a dataset according to the atomic permutational symmetry of the frag-

Table 3
Principal components for four-coordinate Cu complexes.

	PC_1	PC_2	PC_3	PC_4	PC_5	PC_6	PC_7	PC_8	PC_9	$PC_{10}^{(R)}$
(*a*)	Cu^I complexes in T_d symmetry									
% Variance	17.67	17.67	17.67	14.25	14.25	7.78	3.39	3.39	3.39	0.52
IR	T_2	T_2	T_2	E	E	A	T_2	T_2	T_2	A
SDC	S_3,S_4	S_3,S_4	S_3,S_4	S_2	S_2	S_1,S_5	S_3,S_4	S_3,S_4	S_3,S_4	S_1,S_5
(*b*)	Cu(*LL*)*L*′*L*″ complexes in C_{2v} symmetry									
% Variance	27.56	23.92	12.29	10.05	7.79	6.71	4.96	4.45	2.01	0.26
IR	B_1	A_1	A_1	A_1	A_2	B_2	B_1	A_1	B_2	A_1
(*c*)	Cu^{II} complexes in D_{4h} symmetry (16-fold permutation)									
% Variance	19.2	15.8	14.3	14.0	10.4	8.5	8.5	4.2	4.2	0.85
IR	B_{2u}	B_{2g}	A_{1g}	B_{1g}	A_{1g}	E_u	E_u	E_u	E_u	A_{2u}
SDC	S_6	S_3	S_1,S_{01}	S_2	S_1,S_{01}	S_4,S_7	S_4,S_7	S_4,S_7	S_4,S_7	S_5

(R) Component formally redundant.

ment means that the PCs transform as one of the irreducible representations (IR) of the fragment point group, hence the PCs are linear combinations of SDCs belonging to the same IR (Murray-Rust *et al.*, 1978*a*,*b*). The ratio of the coefficients of the SDCs expresses their correlation.[1]

3. Results and discussion

3.1. Copper(I) complexes

Deformations of Cu^I complexes were described with reference to a regular tetrahedral geometry, enumerated as shown in Fig. 1, using the SDCs in Table 1 (Murray-Rust *et al.*, 1978*a*,*b*). Irreducible representations (IR) of the symmetry species of the SDCs in the point group T_d are given, along with the kernel symmetry (minimum point-group symmetry maintained along a deformation coordinate or set of degenerate coordinates) and co-kernel (McDowell, 1965) symmetry (higher symmetry point group maintained along a particular coordinate choice for degenerate coordinates). The PCA results (Table 3*a*) for the normalized bond lengths and angles were uninformative. There is little reduction in dimensionality due to the high symmetry of the reference fragment, as found previously for Cu in all oxidation states (Klebe & Weber, 1994). The first triplet of T_2 coordinates (PC_1–PC_3) account for *ca.* 50% of the variance and the E coordinates (PC_4 and PC_5) *ca.* 30%. SDC plots (Fig. 4) are more useful in describing the predominant deformations, since the angular and bond distance components are separated.

The S_{2a} *versus* S_{2b} plot (Fig. 4*c*) shows that elongation along a D_{2d} coordinate is more common than either D_{2d} compression or a D_2 diagonal twist. For $M(LL)_2$ complexes the restricted bite angle (< 109.5°) of ligands is largely responsible for the apparent elongation. The broadening of the distribution about the elongation pathway indicates that there is a tendency for bidentate ligands to twist in order to adopt a flatter ligand polyhedron when the bite angle of the ligands is reduced. This was apparent for the diagonal twist pathway described by Klebe & Weber (1994), the eight least twisted examples being Cu^I. The tendency for a diagonal twist is increased with large, planar chelating ligands [*e.g.* extended aromatic systems; JARBIN (1), GEVMEZ (2) and GEVNAW(3)]. This twist is probably a packing effect, large torsional forces may be exerted at the copper centre, and is much smaller than that seen in flat Cu^{II} systems.

The T_2 angular and bond distance subspaces may each be described on orthogonal axes in three dimensions, as shown in the three-dimensional scatterplots of S_{3a} *versus* S_{3b} *versus* S_{3c} and S_{4a} *versus* S_{4b} *versus* S_{4c}

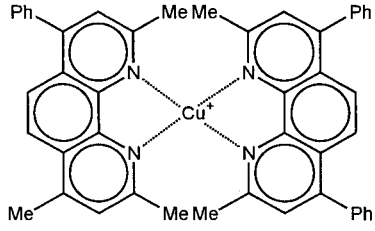

1: JARBIN

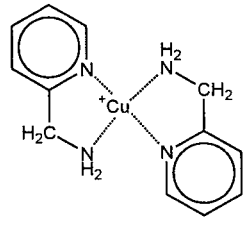

2: GEVMEZ

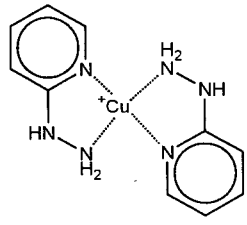

3: GEVNAW

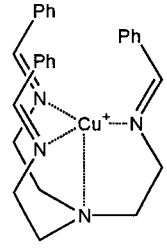

4: JEYVAK

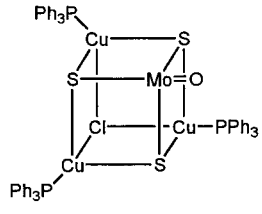

5: YADWIH

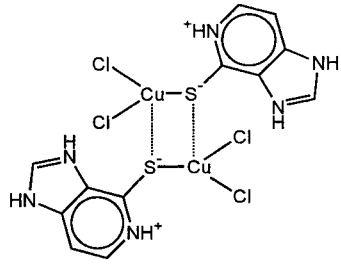

6: MCPURC01

(Fig. 4). Thus, two-dimensional plots of S_{3a} *versus* S_{3b} and S_{4a} *versus* S_{4b} represent projections of these subspaces, perpendicular to the S_{3c} and S_{4c} axes, respectively. The axes

[1] Supplementary data for this paper are available from the IUCr electronic archives (Reference: HA0190). Services for accessing these data are described at the back of the journal.

maintaining C_{3v} co-kernel symmetry (McDowell, 1965) are the body-diagonals of the cube, and an alternative set of SDC axes may be chosen such that one axis maintains C_{3v} co-kernel symmetry (S'_{3a-c} and S'_{4a-c}, Table 1). This corresponds to a rotation of the orthogonal axis set such that one axis coincides with a C_{3v} vector. The S_3 plot (Fig. 4*a*) demonstrates a clear tendency for T_2 bond length deformations to follow a C_{3v} coordinate in a positive sense. This corresponds to the dissociation of a ligand from a tetrahedral complex to form a trigonal planar one. Those outliers that do lie along the S_3 and C_{2v} axes can be attributed to a specific steric effect, *e.g.* clash of α-H atoms in (3).

The T_2 angular deformations (Fig. 4) do not follow such a distinct pattern as the distance component, although there is some preference for C_{2v} or at least C_s symmetry to be maintained. Most of this variation may be ascribed to differing bite angles of chelating ligands. Large deformations on these axes are due largely to the effect of bidentate (C_{2v}) and tridentate (C_{3v}) ligands. Trigonal flattening is observed most commonly in complexes with tripodal ligands, *e.g.* C_6H_4-1,3-$\{CH_2N[(CH_2)_2PPh_2]_2\}_2Cu_2Cl_2$ JOGCEN and $CuN[(CH_2)_2N{=}C(H)Ph]_3$ JEYVAK (4), heterometallic cubanes, *e.g.* YADWIH (5) or dimers of stacked trigonal complexes, *e.g.* MCPURC01 (6) and $Cu_2(\mu_2\text{-}Cl)_2$-$\{S{=}C[N(H)Ph]NHC{=}OCH{=}CHMe\}_4$ SOGZAP. Positive deformations (more pyramidalized) are due typically to the incorporation of the Cu^I atoms into a *pseudo*-cubane core where tridentate ligands are not present, *e.g.* $Cu_4(\mu_3\text{-}Br)_4(PR_3)_4$ clusters BOZRAJ (R = ^{t}Bu) and CUJBEO (R = Ph).

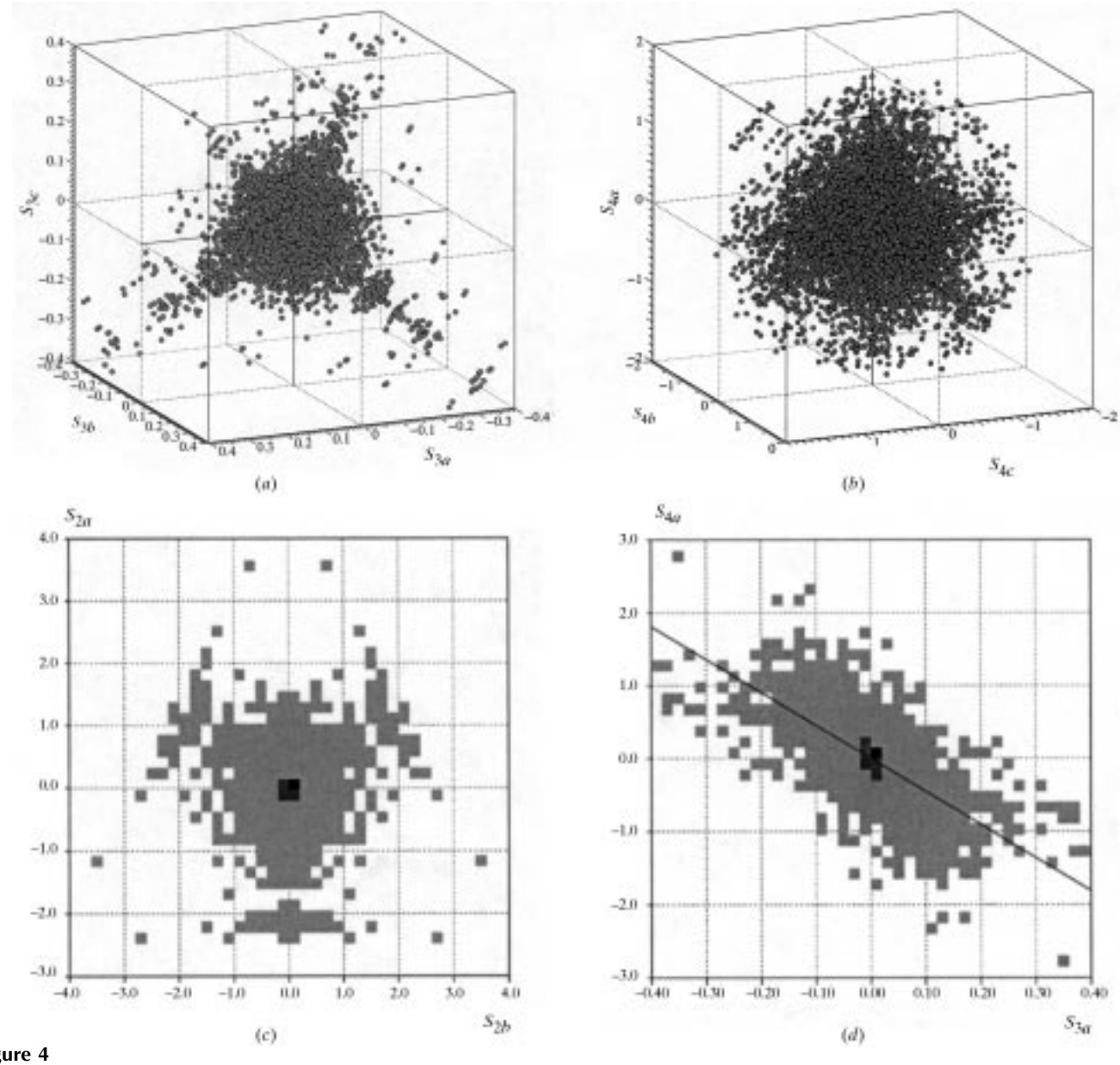

Figure 4
SDC (Table 1) scatterplots for four-coordinate copper(I) complexes. (*a*) S_{3a} *versus* S_{3b} *versus* S_{3c}; (*b*) S_{4a} *versus* S_{4b} *versus* S_{4c}; (*c*) S_{2a} *versus* S_{2b}; (*d*) S_{4a} *versus* S_{3a}.

There is a significant correlation (−0.678) between pairs of angular and bond distance coordinates with T_2 symmetry (Fig. 4*d*), which accounts for the significant coupling of angle and distance components in PC_1–PC_3. (Fig. 5). This demonstrates that there is a tendency for R_1 and R_2 to increase and R_3 and R_4 to decrease, as the corresponding angles θ_{12} decrease and θ_{34} increase, respectively. The PC_1 *versus* PC_2 *versus* PC_3 plot shows some preference for T_2 deformations in three mutually perpendicular directions in the subspace, corresponding to the C_{2v} axes (these are rotated relative to those in the SDC plots), which reflects the predominance of the angular component of the PCs.

To investigate the effect of bidentate ligand bite angle on other monodentate ligands, a subset of Cu(LL)$L'L''$ complexes (where LL is a bidentate ligand, Fig. 1*b*) was studied with reference to T_d SDCs. These were normalized and T_d symmetry-deformation coordinates calculated as before. PCA results are summarized in Table 3(*b*) (bond and angle deformations span the representations $5A_1 \oplus A_2 \oplus 2B_1 \oplus 2B_2$ in C_{2v} symmetry). PC_1 describes a deformation in which the monodentate ligand distances become non-equivalent, *i.e.* a transition from [4] to [3 + 1] geometry. This is exemplified by Cu(CO)(η^1-$OClO_3$)[N,N'-η^2-N(H)(2-py)$_2$] (COJRAU), in which the perchlorate O atom occupies the axial site of a flat trigonal pyramid, maintaining approximate C_{3v} symmetry. PC_2 describes the effect of ligand bite angle. θ_{12} and θ_{34} exhibit a correlation coefficient r = −0.667, *i.e.* A_{12} tends to open as the bite angle of the ligand becomes more restricted. The size and nature of the ligands will determine the extent to which this is so: the extent of opening is dependent on donor atom size, ligand bulk *etc*. These angular deformations are associated with an elongation of R_1 and R_2.

Symmetry-deformation coordinates S_{2a} and S_{2b} show little correlation between elongation (which is usually followed, rather than compression, since the closure of θ_{12} due to small bite angle is not compensated fully by opening of θ_{34}) and twist. That PC_5 accounts for only 7.7% of the variance suggests that the tendency to twist is small and repulsive effects dominate even with ligands with small bite angles; a plot of S_{4a} *versus* S_{2b} shows little correlation between (θ_{12}–θ_{34}) and degree of twist. Similarly, the degree of elongation (S_{2a}) and asymmetry (S_{4a}) are essentially uncorrelated (r = −0.01), although these deformations have the same IR in C_{2v} symmetry. This suggests that the nature of L as well as the bite of ligand LL is important.

S_{3a} and S_{4a} show a much smaller correlation (r = −0.368) than for the full data set and S_{3a} deformations tend to be fairly small, *i.e.* the ligand bite does not have a correlated effect on these metal–ligand bond lengths. Neither does the bite angle affect the degree of dissociation significantly since S_{4a} is not correlated strongly with S_{3b} or S_{3c}. This suggests that the [3 + 1] geometry is not favoured with a chelating ligand (whose bite angle is typically *ca* 90° rather than the 120° suited to trigonal planar coordination). Rather, it may be a function of the relative hardness of the donor atoms and the degree of association in dimers and higher clusters.

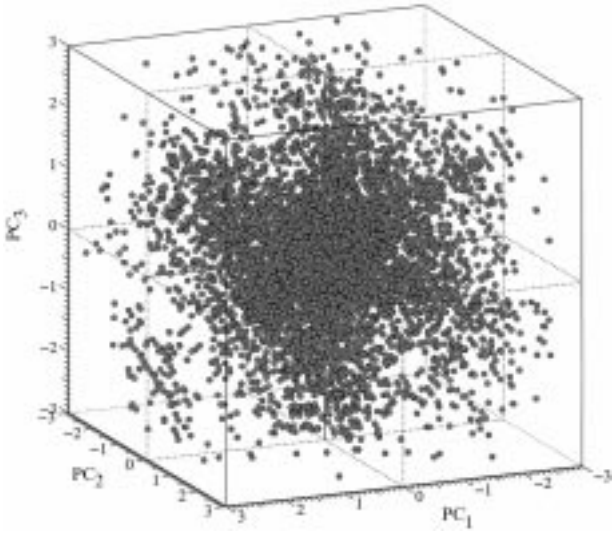

Figure 5
PC scatterplot of PC_1 *versus* PC_2 *versus* PC_3.

3.2. Copper(II) complexes

Since Cu^{II} has a tendency to exhibit planar coordination, a square-planar (D_{4h}) reference geometry was chosen as the basis for deformation studies. Atoms, bonds and angles were defined as shown in Fig. 3 and the SDCs in Table 4 were employed.

The principal components in Table 3(*c*) give an indication of the importance of the symmetry-deformation coordinates, although there is no significant reduction in dimensionality. S_6 (tetrahedral distortion) accounts for almost 20% of the variance and S_3 (restricted bite of ligands) for another 15%. The PC scatterplots obtained are similar in appearance to the SDC plots with the C_{4v} permutation (with twice as many points adding no extra information), although some have an additional mirror plane, a consequence of the σ_h operation generating the other enantiomer of each topological mapping.

The histogram of the mean of angles θ_{13} and θ_{24} (Fig. 6), corresponding to $|S_6|$, shows the degree of deformation from the square-planar to the tetrahedral configuration for the permuted data set. Thus, a (distorted) square-planar geometry predominates for four-coordinate copper(II) complexes in the CSD. Regular tetrahedral geometries are rare and most exhibit some degree of compression. Examination of those entries containing strongly tetrahedrally distorted fragments suggest that the deviation from planar geometry is the result of steric (*e.g.* bulky halogen) or ligand bite (*e.g.* tripodal ligand) requirements.

Complexes with halide ligands tend to show large variations in the extent of tetrahedral distortion. The Cl—Cu—Cl angle distribution for $[CuCl_4]^{2-}$ exhibits a maximum at 133° and a smaller one at 180°, whereas some structures contain nearly tetrahedral anions (Clay *et al.,* 1973). The energy of the highest '*d*–*d*' transition is much greater (13 000 cm^{-1}) in the square-planar than the compressed tetrahedral case (9000 cm^{-1}; Harlow *et al.*, 1974). Correlations between the degree of

Table 4
Symmetry-deformation coordinates (SDCs) for four-coordinate complexes in D_{4h}.

SDC	IR	Kernel	Co-kernel
$S_1 = \frac{1}{2}(\delta R_1 + \delta R_2 + \delta R_3 + \delta R_4)$	A_{1g}†	D_{4h}	
$S_{01} = \frac{1}{2}(\delta\theta_{12} + \delta\theta_{23} + \delta\theta_{34} + \delta\theta_{14})$	A_{1g}†	D_{4h}	
$S_2 = \frac{1}{2}(\delta R_1 - \delta R_2 + \delta R_3 - \delta R_4)$	B_{1g}	D_{2h}	
$S_3 = \frac{1}{2}(\delta\theta_{12} - \delta\theta_{23} + \delta\theta_{34} - \delta\theta_{14})$	B_{2g}	D_{2h}	
$S_{4a} = \frac{1}{(2)^{1/2}}(\delta R_1 - \delta R_3)$	E_u	C_s	C_{2v}
$S_{4b} = \frac{1}{(2)^{1/2}}(\delta R_2 - \delta R_4)$	E_u	C_s	C_{2v}
$S_5 = \frac{1}{(2)^{1/2}}(\delta\theta_{13} + \delta\theta_{24})$	A_{2u}	C_{4v}	
$S_6 = \frac{1}{(2)^{1/2}}(\delta\theta_{13} - \delta\theta_{24})$	B_{2u}	D_{2d}	
$S_{7a} = \frac{1}{(2)^{1/2}}(\delta\theta_{12} - \delta\theta_{34})$	E_u	C_s	C_{2v}
$S_{7b} = \frac{1}{(2)^{1/2}}(\delta\theta_{23} - \delta\theta_{14})$	E_u	C_s	C_{2v}

† The A_{1g} coordinate is S_{01}, which describes the same deformation as S_6, but without any sense of direction (*i.e.* which atoms move above or below the x, y plane of the molecule), is formally redundant. Degenerate SDC axes have been chosen that preserve C_{2v} co-kernel symmetry along each member of a degenerate pair.

compression and the energy of this transition have been investigated by many authors, using either the mean of the two largest angles (Willett *et al.*, 1974; Harlow *et al.*, 1975), the longest opposite edges of the tetrahedron (Lamotte-Brasseur, 1974) or the $Cl_2—Cu—Cl_2$ dihedral angle (Lamotte-Brasseur *et al.*, 1973; Battaglia *et al.*, 1979); a smooth curve was obtained in each case, albeit with careful data selection. Molecular orbital calculations, performed with different basis sets, showed that the most stable configuration was the flattened tetrahedron with 120° Cl—Cu—Cl angle; the flattening was an intrinsic property of the ion (Demuynck *et al.*, 1973). Furthermore, the T_d geometry was found to be more stable than the D_{4h} by *ca* 75 kJ mol^{-1}. Despite the limitations of these calculations and the basis sets employed, the results are in qualitative agreement with experiment.

Complexes in this data set in which one of the Cl ligands has been replaced show similar behaviour. This is consistent with a reasonably flat potential energy surface along this coordinate (S_{2a}). It seems that steric and electronic factors are finely balanced, and the variation observed is due to the influence of small crystal packing forces and hydrogen bonding effects (Lamotte-Brasseur, 1974). The failure to resolve enantiomers

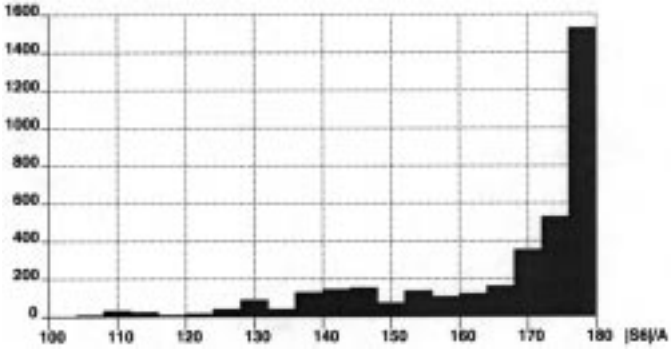

Figure 6
Histogram of mean of angles θ_{12} and θ_{24} (Fig. 3) in copper(II) complexes.

of chiral (flattened) tetrahedral complexes is indicative of their lability; the energy barrier to inversion *via* a square-planar transition state being too small (Harrowfield *et al.*, 1987).

In complexes with bidentate chelating ligands with N or O donor atoms, the square-planar geometry is usually observed. This geometry is particularly favoured if the chelating ligands have (weak) π-acceptor character (*e.g.* unsaturated organic ligands such as acac: Robertson & Truter, 1967) since it allows overlap with the d_{xz} and d_{yz} orbitals to be maximized. However, the presence of bulky side groups leads to a sterically induced distortion, in which the chelating ligands twist whilst maintaining an approximately constant bite angle. This can be seen by comparing similar ligands with substituents of differing steric bulk (Hathaway & Billing, 1970). Whilst [Cu(salim)$_2$] (Baker *et al.*, 1966) is planar, [Cu(^{t}Bu-salim)$_2$] (Morosin & Lingafelter, 1961) has a twisted conformation. Similarly, bis(2,2′-bipyridine) complexes are prevented from assuming a planar arrangement by the steric requirements of the 3,3′ H atoms (Dwyer *et al.*, 1963), *e.g.* in [Cu(bipy)$_2$(ClO$_4$)$_2$] (Hathaway *et al.*, 1969).

The influence of ligand bite on the extent of distortion toward the tetrahedral geometry can be seen in a scatterplot of S_3 *versus* S_6 (Fig. 7*a*). The central portion along S_6 comprises molecules exhibiting varying degrees of tetrahedral distortion in which angles $\theta_{12}, \theta_{23}, \theta_{34}$ and θ_{14} remain equal (the reverse of the T_d S_{2a} coordinate). S_3 shows in-plane deformations in which opposite angles close up (Table 4). This shows the effect of restricted bite angle; the greatest density (darker shading) is concentrated along this axis. There is also a significant density along the diagonals which represent the reverse of the T_d coordinate S_{2b}, the diagonal twist coordinate (along which a pair of opposite angles are constrained by the bite of the ligands; Klebe & Weber, 1994; Muetterties & Guggenberger, 1974). As the complex twists, the degree of tetrahedral distortion and inequality in the adjacent angles in the equatorial plane increases. It seems reasonable that molecules should follow this coordinate, since the bite angle remains approximately constant for inflexible ligands and a symmetric (D_2) twist would minimize repulsion between facing groups.

The initial tetrahedral elongation or rectangular distortion steps suggested in the pathway are probably not followed by a particular molecule. Ring strain effects are important (it is notable that the least distorted square-planar example has six-membered chelate rings, the next five-membered and the most rectangularized in-plane geometry has a four-membered ring). The twist is more favoured sterically with smaller bite angles, although the repulsion between facing ligands is always reduced when twisting away from a planar environment. Hence, a ligand with flexible bite could increase its bite angle on twisting (reducing repulsions between donor atoms in the ligand) instead of reducing it, thus following a coordinate more closely approaching S_{2a}. S_{2b} effectively describes the same deformation as S_{2a}, but with two opposite angles fixed.

Since no tetrahedral Cu^{II} fragments were found with bidentate chelating ligands it would seem that planar mole-

cules are favoured electronically (and possibly also by packing considerations) with twisting occurring only as a consequence of substituent repulsion. Thus, the tetrahedral geometry might be better considered as a higher-energy intermediate or transition-state on a (distorted) square-planar to square-planar geometrical isomerization pathway. In this study, the pathway is only exemplified by structures approaching the lower-energy planar minimum. The results provide no evidence that such an isomerization process occurs, although they are not inconsistent with it.

A plot of S_5 *versus* S_6 (Fig. 7*b*, C_{4v} permutation) indicates that the majority of complexes show little deformation along S_5. A few show deformations in a positive sense with extreme tetrahedral distortion; this occurs when θ_{13} is much further from 180° than θ_{24}, *e.g.* for $[Cu_2Cl_6]^{2-}$ anions (7) (in BOZNEJ, DADZUD, DUBTAV, FINHOZ, FINHUF, FIWWUC and VEJMAY01), other chloro-bridged dimers [*e.g.* JOGKEV (8)] and complexes with tripodal ligands. There is also a cluster with $S_6 \simeq 0$ and S_5 small and negative. This represents complexes in which angles at opposing pairs of donor atoms are very different (*e.g.* alkoxy-bridged dimers) and the coordination geometry is slightly pyramidalized. The absence of any entries at simultaneously large values of S_6 and large negative values of S_5 demonstrates that there is no real tendency for Cu^{II} to adopt a square-pyramidal geometry.

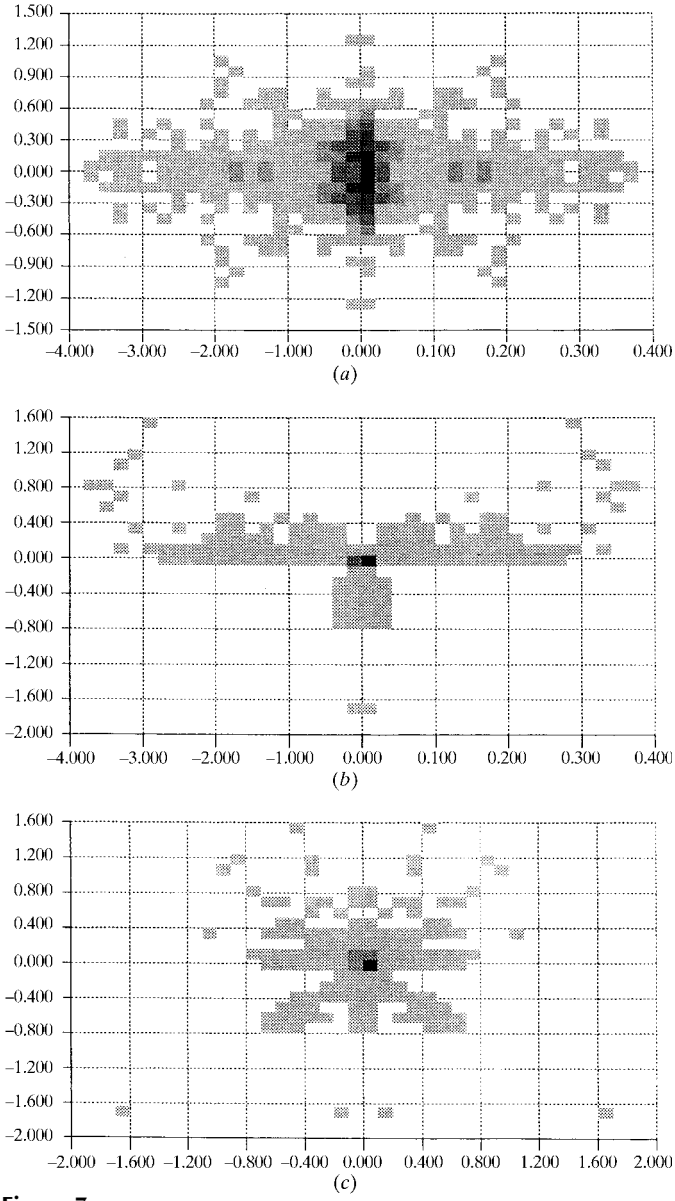

Figure 7
SDC (Table 2) scatterplots for four-coordinate copper(II) for eightfold permuted (C_{4v}) data set. (*a*) S_3 *versus* S_6; (*b*) S_5 *versus* S_6; (*c*) S_5 *versus* S_{7a}.

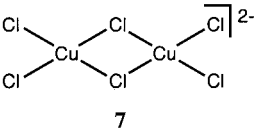

7

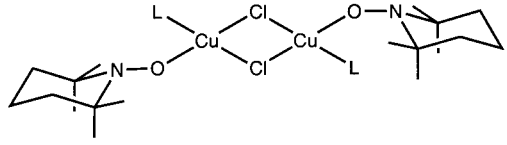

8: JOGKEV

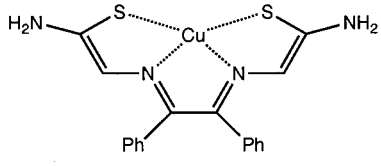

9: BNZSCU01

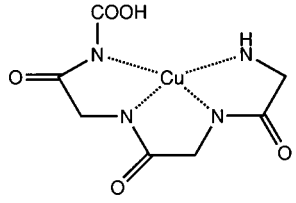

10: NGLYCU

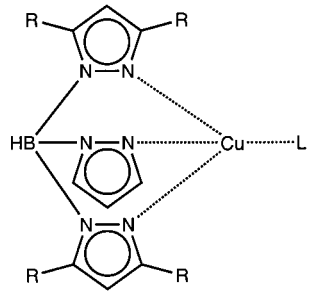

11a-d

The diagonals in the lower half of the plot of S_5 *versus* S_{7a} (Fig. 7*c*) correspond to a closing and opening of opposite angles, whilst the fragment remains almost planar, but slightly pyramidalized. This occurs typically with open-chain tetradentate ligands [*e.g.* BNZSCU01 (9)]. Less correlation is

shown in the upper half of the plot since the degree of tetrahedral distortion (S_6) can vary more widely. No significant correlations exist between S_6 and S_{7a}, except perhaps a tendency for structures with extreme tetrahedral distortion to show a marked non-equivalence in opposite angles [*e.g.* (8) and (11), *see below*]. The density along S_{7a} is due to deformations in the equatorial plane such as those exhibited by (9) and NGLYCU (10) as a result of constraints imposed by their open-chain tetradentate ligands.

No clear pathway is discernible from scatterplots of S_1 *versus* S_2 or S_1 *versus* S_{4a}, although there does appear to be a tendency for overall expansion to occur if the molecule distorts along either S_3 or S_4. This may be due to the asymmetry of the potential energy curve for bond deformation. The effect is evident particularly in the Cl-bridged dimers; the bonds to the bridging Cl ligands are longer than the mean, whilst the terminal bonds are shorter. This is probably due to both the greater repulsion between the bridging as compared with the terminal Cl ligands (bridging angle being constrained and smaller), as well as electronic factors: a halogen does not bond as strongly to each of two copper centres as it does to one alone. There are no large correlations between the angular and bond distance degenerate coordinates either (r = −0.239 for S_{4a} *versus* S_{7a}).

The correlation between S_2 and S_6 is not strong (r = 0.303: these coordinates are not orthogonal under a C_{4v} permutation); most plot density lies along $S_2 = 0$. Those points on a diagonal are mainly due to complexes with tripod ligands and the correlation is exaggerated by those relative outliers, *e.g.* tris(pyrazoyl)borate complexes KETMEB [L = Cl, (11*a*)], PESVOY [L = $OOCMe_2Ph$, (11*b*)], PIBVOL [L = NNC(Ph)C(H)C(Ph), (11*c*)] and SOZKIB [$L = OS(=O)_2CF_3$, (11*d*)]. In these examples, the bond which makes the largest angle (θ_{24}) with the monodentate ligand L (thus experiencing least repulsion) is the shortest, and the bond length to the monodentate ligand L is shorter than the mean for that donor atom in each case, particularly for the bulky chloride ligand in (11*a*). This can be readily interpreted in terms of steric effects; the small bite angles between the N-donor atoms in the tripod ligands provide more space for the fourth ligand.

4. Conclusions

This study has demonstrated that the inorganic chemist's intuitive understanding of the influence of oxidation state on the geometries of four-coordinate Cu complexes is supported by a study of more than 800 structures in the CSD. Furthermore, it has demonstrated that a consideration of oxidation state is fundamental to rationalizing the data, in contrast to the approach of Klebe & Weber (1994).

Symmetry-deformation coordinate analysis has demonstrated that the majority of the four-coordinate copper(I) complexes in the CSD adopt tetrahedral geometries. Deviations from ideal T_d symmetry are due largely to the presence of chelating ligands or the incorporation of the Cu centres into a dimer or larger cluster (*e.g.* a *psuedo*-cubane arrangement). There is no tendency to adopt a more planar configuration in the absence of large planar ligands which are particularly subject to intermolecular interactions in the solid state. Some complexes exhibit a distortion towards a trigonal planar configuration, *i.e.* a C_{3v} [3 + 1] geometry.

Four-coordinate copper(II) complexes generally adopt geometries which approach the square-coplanar stereochemistry. This is particularly true of bis(chelate) complexes, especially where the ligands have π-bonding ability. Deviations toward tetrahedral geometry are usually attributable to steric interactions of bulky substituents on the bidentate ligands. The restricted normalized bite of ligands is responsible for rectangular distortions in planar complexes. Tetra(monodentate) ligand complexes (*e.g.* $[CuCl_4]^{2-}$) display a wider range of stereochemistries; electronic and steric factors are finely balanced and the geometry is sensitive to hydrogen bonding and other intermolecular interactions in the solid state. The potential energy surface is reasonably flat, although a flattened tetrahedral stereochemistry is predicted for a gas-phase molecule.

References

Allen, F. H. & Kennard, O. (1993). *Chem. Des. Autom. News*, **8**, 1, 31–37.

Auf der Heyde, T. P. E. & Bürgi, H.-B. (1989). *Inorg. Chem.* **28**, 3960–3969.

Baker, E. N., Hall, D. & Waters, T. N. (1966). *J. Chem. Soc. A*, pp. 680–684.

Battaglia, L. P., Corradi, A. B., Marcotrigiano, G., Menabue, L. & Pellacani, G. C. (1979). *Inorg. Chem.* **18**, 148–152.

Brown, D. S., Lee, J. D., Melsom, B. G. A., Hathaway, B. J., Procter, I. M. & Tomlinson, A. A. G. (1967). *J. Chem. Soc. Chem. Commun.* pp. 369–371.

Bürgi, H.-B. & Dunitz, J. D. (1991). Editors. *Structure Correlation.* Weinheim: VCH.

Cambridge Structural Database (1992). *Cambridge Structural Database System Users' Manuals.* Cambridge Crystallographic Data Centre, 12 Union Road, Cambridge, England.

Cambridge Structural Database (1994). *Cambridge Structural Database System Users' Manuals.* Cambridge Crystallographic Data Centre, 12 Union Road, Cambridge, England.

Chatfield, C. & Collins, A. J. (1980). *Introduction to Multivariate Analysis.* London: Chapman and Hall.

Clay, R. M., Murray-Rust, P. & Murray-Rust, J. (1973). *J. Chem. Soc. Dalton Trans.* pp. 595–599.

Demuynck, J., Veillard, A. & Wahlgren, U. (1973). *J. Am. Chem. Soc.* **95**, 5563–5574.

Dollase, W. A. (1974). *Acta Cryst.* A**30**, 513–517.

Dwyer, F. P., Goodwin, H. A. & Gyarfas, E. C. (1963). *Aust. J. Chem.* **16**, 544–548.

Gazo, J., Bersuker, I. B., Caraj, J., Kabesova, M., Kohout, J., Langfelderova, H., Melnik, M., Seraton, M. & Valach, F. (1976). *Coord. Chem. Rev.* **19**, 253.

Harlow, R. L., Wells, W. J. III, Watt, G. W. & Simonsen, S. H. (1974). *Inorg. Chem.* **13**, 2106–2111.

Harlow, R. L., Wells, W. J. III, Watt, G. W. & Simonsen, S. H. (1975). *Inorg. Chem.* **14**, 1768–1773.

Harrowfield, J. MacB. & Wild, S. B. (1987). *Comprehensive Coordination Chemistry*, edited by G. Wilkinson, R. D. Gillard and J. A. McCleverty, Vol. 1, pp. 179–212. Oxford: Pergamon Press.

Hathaway, B. J. (1981). *Coord. Chem. Rev.* **35**, 211–252.

Hathaway, B. J. (1982). *Coord. Chem. Rev.* **41**, 423–495.

Hathaway, B. J. & Billing, D. E. (1970). *Coord. Chem. Rev.* **5**, 143–207.
Hathaway, B. J., Duggan, M., Murphy, A., Mullane, J., Power, C., Walsh, A. & Walsh, B. (1981). *Coord. Chem. Rev.* **36**, 267–324.
Hathaway, B. J., Procter, I. M., Slade, R. C. & Tomlinson, A. A. G. (1969). *J. Chem. Soc. A*, pp. 2219–2224.
Holloway, C. E. & Melnik, M. (1995). *Rev. Inorg. Chem.* **15**, 147–386.
Howard, J. A. K., Copley, R. C. B., Yao, J. W. & Allen, F. H. (1998). *Chem. Commun.* pp. 2175–2176.
Jahn, H. A. & Teller, E. (1937). *Proc. R. Soc. London*, **161**, 220–235.
Klebe, G. & Weber, F. (1994). *Acta Cryst.* B**50**, 50–59.
Lamotte-Brasseur, J. (1974). *Acta Cryst.* A**30**, 487–489.
Lamotte-Brasseur, J., Dupont, L. & Dideberg, O. (1973). *Acta Cryst.* B**29**, 241–246.
Makovicky, E. & Balic Zunic, T. (1998). *Acta Cryst.* B**54**, 766–773.
McDowell, R. S. (1965). *J. Mol. Spectrosc.* **17**, 365–367.
Melnik, M., Kabesova, M., DunajJurco, M. & Holloway, C. E. (1997). *J. Coord. Chem.* **41**, 35–182.
Melnik, M., Kabesova, M., Koman, M., Macaskova, L., Garaj, J., Holloway, C. E. & Valent, A. (1998). *J. Coord. Chem.* **45**, 147–359.
Morosin, B. & Lingafelter, E. C. (1961). *J. Phys. Chem.* **65**, 50–51.
Muetterties, E. L. & Guggenberger, L. J. (1974). *J. Am. Chem. Soc.* **96**, 1748–1756.
Murray-Rust, P. & Bland, R. (1978). *Acta Cryst.* B**34**, 2527–2533.
Murray-Rust, P., Bürgi, H.-B. & Dunitz, J. D. (1978*a*). *Acta Cryst.* B**34**, 1787–1793.
Murray-Rust, P., Bürgi, H.-B. & Dunitz, J. D. (1978*b*). *Acta Cryst.* B**34**, 1793–1803.
Murray-Rust, P., Bürgi, H.-B. & Dunitz, J. D. (1979). *Acta Cryst.* A**35**, 703–713.
Orpen, A. G., Brammer, L. L., Allen, F. H., Kennard, O., Watson, D. G. & Taylor, R. (1989). *J. Chem. Soc. Dalton Trans.* pp. S1–S83.
Pauling, L. (1940). *Nature of the Chemical Bond*, 2nd ed. Oxford University Press.
Pinsky, M. & Avnir, D. (1998). *Inorg. Chem.* **37**, 5575–5582.
Robertson, I. & Truter, M. R. (1967). *J. Chem. Soc. A*, pp. 309–313.
Smith, D. R. (1997*a*). *Coord. Chem. Rev.* **162**, 155–240.
Smith, D. R. (1997*b*). *Coord. Chem. Rev.* **164**, 575–666.
Smith, D. R. (1998). *Coord. Chem. Rev.* **172**, 457–573.
Smith, D. W. (1995). *Ann. Rep. Prog. Chem. A*, **92**, 227–245.
Smith, D. W. (1996). *Ann. Rep. Prog. Chem. A*, **93**, 221–239.
Smith, D. W. (1997). *Ann. Rep. Prog. Chem. A*, **94**, 233–253.
Toh, K. H. (1994). *PLOTMTV*, Version 1.4. Technology CAD, Intel Corporation, 2200 Mission College Boulevard, Santa Clara, California, USA.
Willett, R. D., Haugen, J. A., Lebsack, J. & Morrey, J. (1974). *Inorg. Chem.* **13**, 2510–2513.